

Zeitschrift: Helvetica Physica Acta
Band: 60 (1987)
Heft: 5-6

Artikel: Recent progress in hyperon physics
Autor: Extermann, Pierre
DOI: <https://doi.org/10.5169/seals-115870>

Nutzungsbedingungen

Die ETH-Bibliothek ist die Anbieterin der digitalisierten Zeitschriften. Sie besitzt keine Urheberrechte an den Zeitschriften und ist nicht verantwortlich für deren Inhalte. Die Rechte liegen in der Regel bei den Herausgebern beziehungsweise den externen Rechteinhabern. [Siehe Rechtliche Hinweise.](#)

Conditions d'utilisation

L'ETH Library est le fournisseur des revues numérisées. Elle ne détient aucun droit d'auteur sur les revues et n'est pas responsable de leur contenu. En règle générale, les droits sont détenus par les éditeurs ou les détenteurs de droits externes. [Voir Informations légales.](#)

Terms of use

The ETH Library is the provider of the digitised journals. It does not own any copyrights to the journals and is not responsible for their content. The rights usually lie with the publishers or the external rights holders. [See Legal notice.](#)

Download PDF: 13.10.2024

ETH-Bibliothek Zürich, E-Periodica, <https://www.e-periodica.ch>

RECENT PROGRESS IN HYPERON PHYSICS

Pierre Extermann, University of Geneva

Since high-energy hyperon beams became operational both at Fermilab (about 1972) and at the CERN SPS (1976), a large set of new and accurate data was produced [1,2]. These results can be summarized in the following way.

1) Hyperon inclusive production in high-energy proton nucleus collisions. The invariant production cross sections have been measured as a function of x_F and p_t . Furthermore, sizeable hyperon polarisations were observed for Σ^+ , Σ^- , Λ , Ξ^0 and Ξ^- .

2) Magnetic moments. Taking advantage of this polarisation, accurate measurements of the Σ^+ , Σ^- , Λ , Ξ^0 and Ξ^- magnetic moments have been performed. A measurement of the Ω^- polarisation and if possible of the Ω^- magnetic moment is under way at Fermilab.

3) Hyperon decays. Nonleptonic, semileptonic and radiative decays have been measured. For semileptonic decays, the Cabibbo theory was found to provide an excellent description of the n , Λ , Σ^- and Ξ^- decays.

4) Hyperon induced reactions. Hyperons, mostly Σ^- and Ξ^- , were used as projectiles on various targets. The following processes were investigated :

i) charmed baryon production. The Ξ_C^+ (former A^+) was discovered and an indication for the Ω_C^0 (T^0) was obtained.

ii) resonance production. The main emphasis was put on Ξ^* and Ω^* spectroscopy. The first Ω^* resonances were observed [3] as well as several Ξ^* resonances.

iii) inclusive processes, e.g. Ξ^- and Ω^- production.

iv) search for new particle types. A still unexplained signal, X(3100) (or U), carrying the numbers $B = 0$ and $S = -1$, was observed in three different charge states.

v) hyperon-nucleon total cross sections and elastic differential cross sections. The Σ^- nucleon and Ξ^- nucleon total cross sections were measured with an accuracy better than 1%.

In this talk, I shall concentrate on a single item, the radiative decays. These decays have branching ratios of the order of 10^{-3} , like the semileptonic decays. Furthermore, most radiative decay modes (e.g. $\Lambda \rightarrow n\gamma$) have a competing nonleptonic decay mode (e.g. $\Lambda \rightarrow n\pi^0$) with a π^0 in the final state which can fake radiative decays when one of the γ s from the π^0 escapes detection. A very good understanding of the photon detectors is required in order to suppress this background.

As an example, let us consider the measurement of the $\Lambda \rightarrow n\gamma$ decay [4]. This experiment was performed with the CERN-SPS hyperon beam Y1 [5]. Basically, the experimental apparatus consisted of a two-stage magnetic spectrometer equipped with proportional and drift chambers, and of two photon detectors, a liquid argon calorimeter (LAD) located at the far end of the experiment and a window-frame lead glass array (LG) placed upstream of the second magnet. Longitudinal sampling in the LAD allowed electromagnetic showers to be separated from hadronic showers. A set of scintillation counters and hodoscopes was used for triggering.

The Λ s used in this experiment originated from $\Xi^- \rightarrow \Lambda\pi^-$ decays. The hyperon beam was tuned at 116 GeV/c and the differential Cherenkov counter (DISC) was set to trigger on Ξ^- . The π^- momentum was measured in the first stage of the spectrometer and the Λ momentum was computed from the decay kinematics. (Note that the polarisation of the Λ was readily available and could have been used for the measurement of the α parameter.)

The energy of the photon, E_γ , as well as the transverse coordinates x_γ and y_γ of its impact point were measured in the LAD. The transverse coordinates of the neutron, x_n and y_n , were also determined in the LAD. From these data, the kinematics of the $\Lambda \rightarrow n\gamma$ decay was computed and the z coordinate of the Λ decay point was determined.

The background came predominantly from $\Lambda \rightarrow n\pi^0$, $\pi^0 \rightarrow \gamma(\gamma)$ events where one of the γ s escaped detection. For instance, this γ could miss the LAD and the LG altogether, or it could hit the LAD in the vicinity of the neutron in which case the two showers merged, or its energy was low and the resulting shower was too small to be found by the pattern recognition program.

In short, the background rejection method was as follows. The LG wall was used as a veto. A minimum transverse distance between two showers in the LAD was required in order to ensure a clean measurement of the photon energy. A Monte-Carlo simulation of both decay modes ($\Lambda \rightarrow n\gamma$ and $\Lambda \rightarrow n\pi^0$, $\pi^0 \rightarrow \gamma\gamma$) allowed to define a "signal region" in the (E_γ, z_Λ) plane (see fig. 1a and fig. 1b). All events in this region and in a band surrounding it were visually scanned on a computer printout and the energy pattern in the LAD was examined for extra or dubious showers. Finally, since neither electromagnetic nor hadronic showers were simulated in the Monte Carlo, the resolutions were checked on a sample of fully reconstructed $\Lambda \rightarrow n\pi^0$ events.

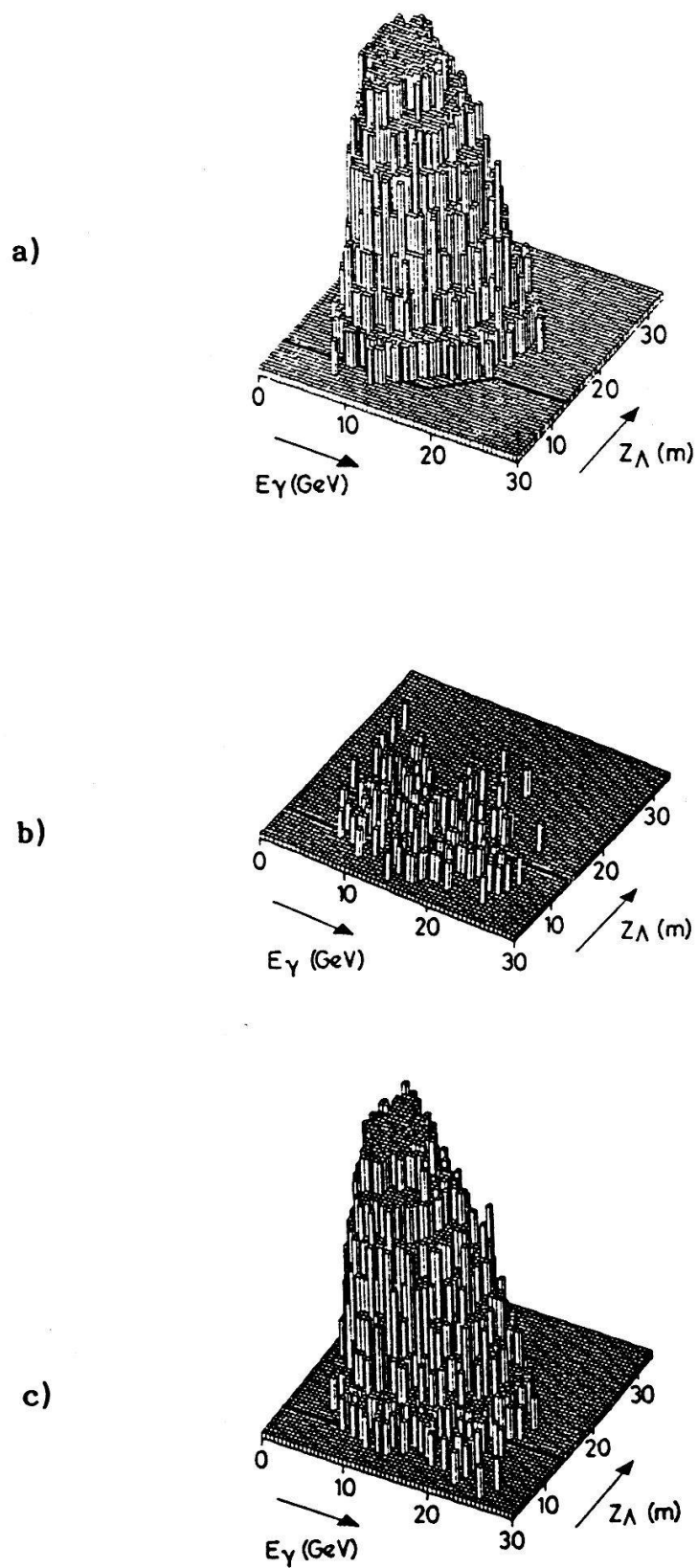


Figure 1 a) $\Lambda \rightarrow n\gamma(\gamma)$ events (M.C.) b) $\Lambda \rightarrow n\gamma$ events (M.C.)
c) Data

The distribution of the data, after the scanning procedure, is shown in fig. 1c. The signal region contains 31 events (42 before scanning). The background in this region is estimated to be 7.3 events. Therefore the net signal is 23.7 events, which corresponds to a branching ratio

$$BR = \frac{\Gamma(\Lambda \rightarrow n\gamma)}{\Gamma(\Lambda \rightarrow \text{all})} = (1.02 \pm 0.33) \times 10^{-3}$$

where the error contains both statistical and systematic contributions. It turns out that the statistics of this final sample is too small for any significant measurement of the asymmetry parameter $\alpha(\Lambda \rightarrow n\gamma)$.

The present experimental status of hyperon radiative decays is summarized in Table 1. For comparison, the 1978 situation is also indicated.

TABLE 1
HYPERON RADIATIVE DECAYS
EXPERIMENTAL DATA

A) <u>Branching ratios</u> (in units of 10^{-3})			
	(1978) [6]	(1987)	
$\Sigma^+ \rightarrow p\gamma$	1.24 ± 0.18	1.22 ± 0.10	[7]
$\Lambda \rightarrow n\gamma$		1.02 ± 0.33	[4]
$\Xi^0 \rightarrow \Sigma^0\gamma$	< 70	< 70	[7]
$\Xi^0 \rightarrow \Lambda\gamma$	50 ± 50	1.3 ± 0.2	[8]
$\Xi^- \rightarrow \Sigma^-\gamma$	< 1.2	0.23 ± 0.10	[9]
$\Omega^- \rightarrow \Xi^-\gamma$		< 2.2	[10]
B) <u>Asymmetries</u>			
		+ 0.52	
$\Sigma^+ \rightarrow p\gamma$	- 1.03	- 0.72 \pm 0.29	[7]
		- 0.42	

The value of the $\Xi^0 \rightarrow \Lambda\gamma$ branching ratio is still preliminary and the quoted error is purely statistical. The progress made over the last decade is almost entirely due to hyperon beam experiments. Note that a new measurement of $\alpha(\Sigma^+ \rightarrow p\gamma)$ has been undertaken at K.E.K. in a low energy pion beam [11].

On the theoretical side, several attempts have been made to compute the rates and asymmetries of hyperon radiative decays [12] but, to put it bluntly, there is as yet no adequate description of these processes. The obvious stumbling block is the strong interactions of the quarks within the baryons. Two approaches are used, one at the quark level (see some examples in fig. 2a) and the other at the hadron level (fig. 2b). Sometimes both approaches are combined. Photon emission is occurring either over short distances ($\sim 1/M_W$) or over large distances (\sim confining radius). Standard techniques are used for the computation of the matrix elements such as bag models, SU(6) wave functions, current algebra, etc.. A few representative results are given in Table 2. Kogan and Shifman [12] computed the Ξ^- and Ω^- decays using a diagram with two hadrons in the intermediate state, $\Lambda\pi^-$ and $\Xi^0\pi^-$ respectively. For the Σ^+ decay, they used the usual pole diagram. Their results are in good agreement with the experimental data. They also obtain an exact lower unitary bound for the decay branching ratios. Eeg [13] used Penguin diagrams, bags and pole models to compute the Ω^- decay rate. His values are well compatible with the experimental upper limit. Kamal and Verma [14] compute diagrams in which the transition mechanism involves 1, 2 or 3 quark lines. They obtain two solutions, labelled A and B, using as an input the Σ^+ and Ξ^- rates and the Σ^+ asymmetry. Their original solution B is shown in Table 2, along with a new solution B' obtained by us from the up-to-date values of the Σ^+ , Λ and Ξ^- decay rates. The agreement with the data is good but the contribution of the single quark line mechanism is much too strong according to several authors [12].

TABLE 2.
Radiative Branching Ratios
(in units of 10^{-3})

	$\Sigma^+ \rightarrow p\gamma$	$\Lambda \rightarrow n\gamma$	$\Xi^0 \rightarrow \Lambda\gamma$	$\Xi^- \rightarrow \Sigma^-\gamma$	$\Omega^- \rightarrow \Xi^-\gamma$
Data	1.22 ± 0.34	1.02 ± 0.33	1.3 ± 0.20	0.23 ± 0.10	< 2.2
Theory :					
(a few examples)					
Kogan & Shifman	~ 1			0.17	0.01 - 0.015
Unitary limit	≥ 0.03			≥ 0.1	≥ 0.008
Eeg [13]					0.001 - 0.1
Kamal (B) & Verma (B')	1.24 1.22	1.70 1.02	1.36 1.04	1.20 0.23	0.6 0.12

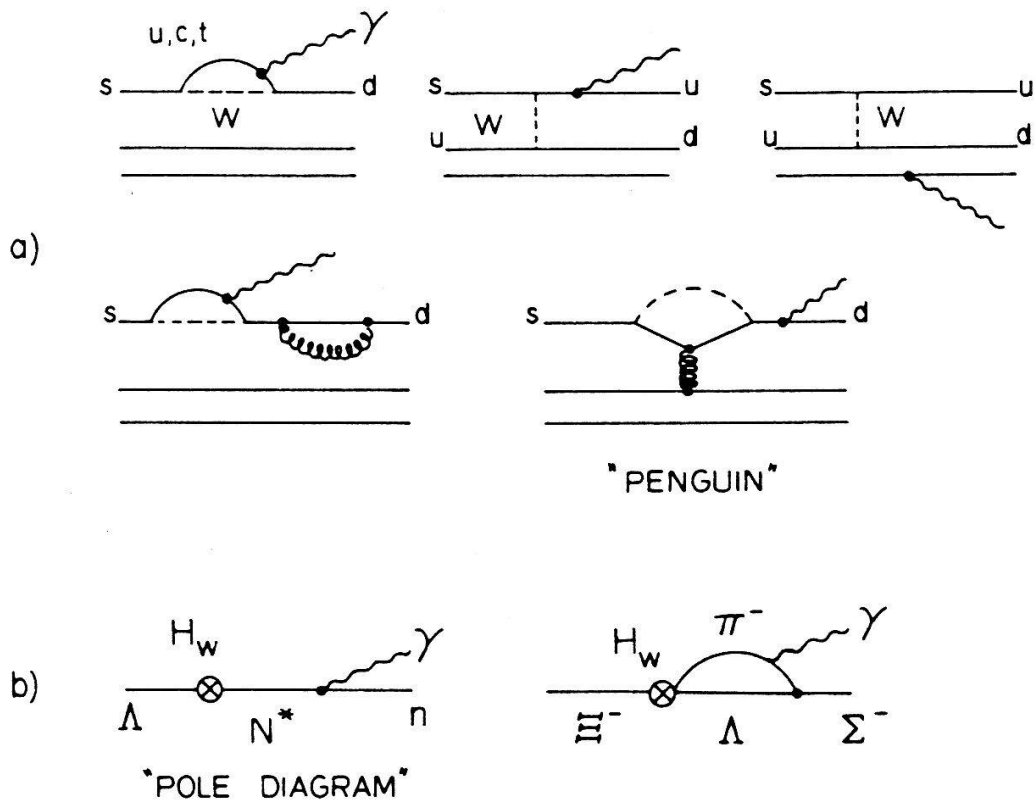


Figure 2 Diagrams for radiative decays

In conclusion, hyperon radiative decays represent a fine challenge for experimentalists and a powerful test bench for theorists. On the experimental side, substantial progress was achieved thanks to the high-energy hyperon beams, but most decay asymmetries are still unmeasured. They are urgently needed to compare parity-violating and parity-conserving amplitudes. On the theoretical side, a lot of work has been done but the computations of the matrix elements on the basis of the quark diagrams are handicapped by QCD effects and are not yet reliable. Models with intermediate hadronic states and pole diagrams yield estimates which should be correct to within a factor 2 to 10. Therefore work should be pursued on either side, experimental and theoretical, in order to reach a full understanding of this physical process.

REFERENCES

- [1] M. Bourquin and J.P. Repellin, Phys. Reports 114, 99 (1984).
- [2] L.G. Pondrom, Phys. Reports 122, 57 (1985).
- [3] S.F. Biagi et al., Z. Phys. C 31, 33 (1986).
- [4] S.F. Biagi et al., Z. Phys. C 30, 201 (1986).
- [5] M. Bourquin et al., Nucl. Phys. B153, 13 (1979).
- [6] Particle Data Group, Phys. Letters 75B, 1 (1978).
- [7] Particle Data Group, Phys. Letters 170B, 1 (1986).
- [8] M. Gilchriese, Rapporteur's talk, XXIII Intern. Conf. on High Energy Physics, Berkeley, 1986.
- [9] S.F. Biagi et al. Accepted for publication by Z. für Physik (1987).
- [10] M. Bourquin et al., Nucl. Phys. B241, 1 (1984).
- [11] Experiment 92, KEK.
- [12] Ya.I. Kogan and M.A. Shifman, Sov. J. Nucl. Phys. 38, 628 (1983) and references therein.
- [13] J.O. Eeg, Z. Phys. C 21, 253 (1984).
- [14] A.N. Kamal and R.C. Verma, Phys. Rev. D26, 190 (1982).

* * * * *